



HAL
open science

Unified H_∞ Observer for a Class of Nonlinear Lipschitz Systems: Application to a Real ER Automotive Suspension

Thanh-Phong Pham, Olivier Sename, Luc Dugard

► **To cite this version:**

Thanh-Phong Pham, Olivier Sename, Luc Dugard. Unified H_∞ Observer for a Class of Nonlinear Lipschitz Systems: Application to a Real ER Automotive Suspension. IEEE Control Systems Letters, 2019, 3 (4), pp.817-822. 10.1109/LCSYS.2019.2919813 . hal-02160053

HAL Id: hal-02160053

<https://hal.science/hal-02160053v1>

Submitted on 19 Jun 2019

HAL is a multi-disciplinary open access archive for the deposit and dissemination of scientific research documents, whether they are published or not. The documents may come from teaching and research institutions in France or abroad, or from public or private research centers.

L'archive ouverte pluridisciplinaire **HAL**, est destinée au dépôt et à la diffusion de documents scientifiques de niveau recherche, publiés ou non, émanant des établissements d'enseignement et de recherche français ou étrangers, des laboratoires publics ou privés.

Unified \mathcal{H}_∞ Observer for a Class of Nonlinear Lipschitz Systems: application to a real ER Automotive Suspension*

Thanh-Phong Pham^{1,2}, Olivier Sename¹, and Luc Dugard¹

Abstract—This paper presents an extension of the synthesis of a unified \mathcal{H}_∞ observer for a specific class of nonlinear systems. The objectives are to decouple the effects of bounded unknown input disturbances and to minimize the effects of measurement noises on the estimation errors of the state variables by using \mathcal{H}_∞ criterion, while the nonlinearity is bounded through a Lipschitz condition. This new method is developed to estimate the damping force of an Electro-Rheological (ER) damper in an automotive suspension system, and is implemented on the INOVE testbench from GIPSA-lab (1/5-scaled real vehicle) for real-time performance assessment. Both simulation and experimental results demonstrate the effectiveness of the proposed observer to estimate the damper force in real-time, face to measurement noises and road disturbances.

I. INTRODUCTION

Nowadays, semi-active suspensions are widespread in vehicle applications because of their advantages compared to active and passive suspensions (see [1] and references therein). A review about control approaches is presented in [2]. Some control approaches considered the damper force as the control input of the suspension system, and then use an inverse model or look-up tables for implementation (see for instance [3], [4], [5]). Others use the force tracking control schemes for local controller in order to attain control objectives [6]. Therefore, the damper force signal is crucial for control and diagnosis of suspension systems.

To fulfill the demand, several estimation methodologies were proposed to estimate the damper force in real-time. It is worth noting that the damper force measurements are difficult and expensive, so the methods should use classical on-board sensors. Moreover the method must take the dynamic behavior of damper into account, and deal with the nonlinearity in presence of unknown road disturbances and sensor noises. Kalman filters were used in [7] to estimate the damper force while ignoring the dynamic characteristic of the semi-active damper. In [8], the authors proposed an H_∞ damping force observer based on a dynamic nonlinear model of the ER damper, while three sensors are required

as inputs of the observer. To handle the nonlinearity and maintain the consideration of dynamic characteristic of MR damper, an LPV- H_∞ based approach is introduced in [9] using the deflection and deflection velocity data (which are costly and not common sensors) to compute the scheduling parameter.

To overcome the above issue, the LMI-based observer for Lipschitz nonlinear systems is a potential approach since the nonlinearity in the ER model satisfies the Lipschitz condition. Over the last decade, there have been several theoretical research contributions for observer design of Lipschitz nonlinear systems (see [10]–[14]). The above-mentioned methodologies are broadly classified into a) Proportional Observers and b) Proportional-Integral Observers. More recently, this has been extended to propose a unified form of the dynamic observer for linear systems in [15], and for Lipschitz systems in the absence of unknown inputs in [16].

In this paper, we aim first to extend the unified observer in [15] to Lipschitz systems in the presence of sensor noises and unknown input disturbances based on the \mathcal{S} -procedure lemma. Then this observer is developed in order to estimate the damper force of an ER damper in automotive suspension, using two accelerometers only. A nonlinear suspension model of a quarter-car vehicle model is augmented with a first order dynamical nonlinear damper model, which captures the main behavior of the ER suspension system.

The two major contributions of this paper are as follows:

- A unified \mathcal{H}_∞ observer for Lipschitz nonlinear system in presence of unknown disturbances and measurement noises is developed minimizing, in an \mathcal{L}_2 -induced gain objective, the effect of sensor noises and decoupling unknown disturbances.
- The proposed observer has been implemented on a real scaled-vehicle test bench, through the Matlab/Simulink real-time workshop. The observer performances are then assessed with experimental tests

The rest of this paper is as follows. Section II presents the problem formulation and III the design of the unified \mathcal{H}_∞ observer. In section IV this method is applied to the real ER automotive suspension system. Section V gives some concluding remarks.

II. PROBLEM FORMULATION

Consider the nonlinear Lipschitz system described by

$$\begin{cases} \dot{x} &= Ax + B\Phi(x)u + D_1\omega_r \\ y &= Cx + D_2\omega_n \end{cases} \quad (1)$$

*This work has been partially supported by the 911 scholarship from Vietnamese government. The authors also thank the financial support of the ITEA 3, 15016 EMPHYSIS project

Thanh-Phong Pham is with Univ. Grenoble Alpes, CNRS, Grenoble INP[†], GIPSA-lab, 38000 Grenoble, France. (e-mail: thanh-phong.pham2@gipsa-lab.grenoble-inp.fr) and Faculty of Electrical and Electronic Engineering, The University of Danang - University of Technology and Education, 550000 Danang, Vietnam (e-mail: pthong@ute.udn.vn).

Olivier Sename and Luc Dugard are with Univ. Grenoble Alpes, CNRS, Grenoble INP[†], GIPSA-lab, 38000 Grenoble, France (e-mail: {olivier.sename;luc.dugard}@gipsa-lab.grenoble-inp.fr). [†]Institute of Engineering Univ. Grenoble Alpes

where $x \in \mathbb{R}^n$, $u \in \mathbb{R}^m$, $\omega_r \in \mathbb{R}^l$, and $\omega_n \in \mathbb{R}^f$ are state, control input, unknown disturbance input and measurement noise input vectors respectively. Matrices A , B , D_1 , C and D_2 are known and of appropriate dimensions.

Assumptions:

A1) The nonlinearity $\Phi(x)$ is globally Lipschitz in x , i.e.: $\forall x, \hat{x} \in \mathbb{R}^n$

$$\|\Phi(x) - \Phi(\hat{x})\| \leq \gamma \|x - \hat{x}\|, \forall x, \hat{x} \quad (2)$$

where γ is called the Lipschitz constant, which, according to [11], [17], is rewritten here as (with Γ a constant matrix)

$$\|\Phi(x) - \Phi(\hat{x})\| \leq \|\Gamma(x - \hat{x})\|, \forall x, \hat{x}. \quad (3)$$

A2) The control input is bounded $|u_i| \leq U_i$ with $i = 1, \dots, m$, $U := [U_1 \dots U_m]^T$. In practice, the known control input signal U is bounded due to the power limitation.

The form of a unified H_∞ observer is given by

$$\begin{cases} \dot{z} = Nz + Jy + H\Phi(\hat{x})u + Mv \\ \dot{v} = Pz + Qy + Gv \\ \hat{x} = Rz + Sy \end{cases} \quad (4)$$

where $z \in \mathbb{R}^n$ is the state variable of the observer, $v \in \mathbb{R}^n$ is the auxiliary vector, $\hat{x} \in \mathbb{R}^n$ is the estimated state variables. All matrices $N, J, H, M, P, Q, G, R, S$ of appropriate dimensions are the observer matrices to be designed.

The dynamic error is given as

$$\epsilon = z - Tx. \quad (5)$$

where the matrix $T \in \mathbb{R}^{n \times n}$ is an arbitrary matrix.

Differentiating (5) with respect to time and using (1) and (4), one obtained:

$$\begin{cases} \dot{\epsilon} = N\epsilon + (NT - TA + JC)x - TD_1\omega_r + JD_2\omega_n \\ \quad + (H - TB)\Phi(\hat{x})u - TB(\Phi(x) - \Phi(\hat{x}))u + Mv \\ \dot{v} = P\epsilon + (PT + QC)x + QD_2\omega_n + Gv \\ \hat{x} = R\epsilon + (RT + SC)x + SD_2\omega_n. \end{cases} \quad (6)$$

Denote $\zeta = \begin{pmatrix} \epsilon \\ v \end{pmatrix}$, equations (6) become

$$\begin{cases} \dot{\zeta} = \begin{pmatrix} N & M \\ P & G \end{pmatrix} \zeta + \begin{pmatrix} NT - TA + JC \\ PT + QC \end{pmatrix} x + \begin{pmatrix} TD_1 \\ 0 \end{pmatrix} \omega_r \\ \quad + \begin{pmatrix} H - TB \\ 0 \end{pmatrix} \Phi(\hat{x})u - \begin{pmatrix} TB \\ 0 \end{pmatrix} \Delta\Phi \cdot u + \begin{pmatrix} JD_2 \\ QD_2 \end{pmatrix} \omega_n \\ \hat{x} = \begin{pmatrix} R & 0 \end{pmatrix} \zeta + (RT + SC)x + SD_2\omega_n \end{cases} \quad (7)$$

where $\Delta\Phi = \Phi(x) - \Phi(\hat{x})$.

It is obvious that if the following conditions are satisfied:

$$NT - TA + JC = 0 \quad (8)$$

$$TD_1 = 0 \quad (9)$$

$$H - TB = 0 \quad (10)$$

$$PT + QC = 0 \quad (11)$$

$$RT + SC = I \quad (12)$$

the system (7) becomes

$$\begin{cases} \dot{\zeta} = \begin{pmatrix} N & M \\ P & G \end{pmatrix} \zeta - \begin{pmatrix} TB \\ 0 \end{pmatrix} \Delta\Phi \cdot u + \begin{pmatrix} JD_2 \\ QD_2 \end{pmatrix} \omega_n \\ e = \begin{pmatrix} R & 0 \end{pmatrix} \zeta + SD_2\omega_n \end{cases} \quad (13)$$

where $e = \hat{x} - x$ is the estimation error.

The problem of the unified \mathcal{H}_∞ observer design reduces to determine observer matrices $N, J, H, M, P, Q, G, R, S$ such that all conditions (8)-(12) are satisfied and the effect of measurement noise ω_n on estimation error e is minimized while $\Delta\Phi \cdot u$ is bounded.

A. Parameterization of the observer matrices

In order to determine the observer matrices T, P, Q, R, S, H, N, J of the proposed observer satisfying all the conditions equalities (8)-(12), the parameterisation is made by using the general solution of (8)-(12) as explained in [15].

Firstly, from equations (11) and (12), one obtained

$$\begin{pmatrix} P & Q \\ R & S \end{pmatrix} \begin{pmatrix} T \\ C \end{pmatrix} = \begin{pmatrix} 0 \\ I \end{pmatrix}. \quad (14)$$

The equation (14) is solvable if and only if

$$\text{rank} \begin{pmatrix} T \\ C \\ 0 \\ I \end{pmatrix} = \text{rank} \begin{pmatrix} T \\ C \end{pmatrix} = n. \quad (15)$$

Next, let matrix $E \in \mathbb{R}^{n \times n}$ be an arbitrary matrix of full row rank such that:

$$\text{rank} \begin{pmatrix} E \\ C \end{pmatrix} = \text{rank} \begin{pmatrix} T \\ C \end{pmatrix} = n. \quad (16)$$

Then there always exists a parameter matrix K such that:

$$\begin{pmatrix} T \\ C \end{pmatrix} = \begin{pmatrix} I & -K \\ 0 & I \end{pmatrix} \begin{pmatrix} E \\ C \end{pmatrix} \Leftrightarrow T = E - KC. \quad (17)$$

Consequently, equation (14) becomes:

$$\begin{pmatrix} P & Q \\ R & S \end{pmatrix} \begin{pmatrix} I & -K \\ 0 & I \end{pmatrix} \begin{pmatrix} E \\ C \end{pmatrix} = \begin{pmatrix} 0 \\ I \end{pmatrix}. \quad (18)$$

and there exists an exact solution set fulfilling (18), in the form of

$$\begin{pmatrix} P & Q \\ R & S \end{pmatrix} = \left[\begin{pmatrix} 0 \\ I \end{pmatrix} \Sigma^+ - Y_m (I - \Sigma \Sigma^+) \right] \begin{pmatrix} I & K \\ 0 & I \end{pmatrix} \quad (19)$$

where $\Sigma = \begin{pmatrix} E \\ C \end{pmatrix}$, Σ^+ is any general inverse of matrix Σ satisfying $\Sigma \Sigma^+ \Sigma = \Sigma$, Y_m is a free matrix of appropriate dimension. This is equivalent to:

$$P = -Y_{m1}\beta_1, \quad Q = -Y_{m1}\beta_2, \quad (20)$$

$$R = \alpha_1 - Y_{m2}\beta_1, \quad S = \alpha_2 - Y_{m2}\beta_2 \quad (21)$$

with $Y_{m1} = (I \ 0)Y_m$, $Y_{m2} = (0 \ I)Y_m$, $\alpha_1 = \Sigma^+ \begin{pmatrix} I \\ 0 \end{pmatrix}$, $\alpha_2 = \Sigma^+ \begin{pmatrix} K \\ I \end{pmatrix}$, $\beta_1 = (I - \Sigma\Sigma^+) \begin{pmatrix} I \\ 0 \end{pmatrix}$, $\beta_2 = (I - \Sigma\Sigma^+) \begin{pmatrix} K \\ I \end{pmatrix}$.

Besides, from the equations (9) and (17), one obtained

$$KCD_1 = ED_1 \quad (22)$$

which can be solved if and only if

$$\text{rank} \begin{pmatrix} ED_1 \\ CD_1 \end{pmatrix} = \text{rank} \left[\begin{pmatrix} E \\ C \end{pmatrix} D_1 \right] = \text{rank} D_1 = \text{rank} CD_1. \quad (23)$$

there exists one solution of (22), as follows

$$K = ED_1(CD_1)^+. \quad (24)$$

From the condition (10), one obtains

$$H = TB = (E - KC)B = (E - ED_1(CD_1)^+C)B. \quad (25)$$

On the other hand, substituting (17) into the decoupling condition (8), one obtains

$$\begin{aligned} N(E - KC) - (E - KC)A + JC &= 0 \\ \Leftrightarrow (N \ J - NK) \Sigma &= (E - ED_1(CD_1)^+C)A \end{aligned} \quad (26)$$

which can also be parameterized as

$$(N \ K_1) \Sigma = \Theta \quad (27)$$

where

$$K_1 = J - NK, \Theta = (E - ED_1(CD_1)^+C)A. \quad (28)$$

and the solution set of (27) is given by

$$(N \ K_1) = \Theta\Sigma^+ - Y_{m3}(I - \Sigma\Sigma^+) \quad (29)$$

which is equivalent to

$$N = \alpha_3 - Y_{m3}\beta_1 \quad (30)$$

$$K_1 = \alpha_4 - Y_{m3}\beta_3 \quad (31)$$

where Y_{m3} is a free matrix of appropriate dimension and

$$\alpha_3 = \Theta\Sigma^+ \begin{pmatrix} I \\ 0 \end{pmatrix}, \alpha_4 = \Theta\Sigma^+ \begin{pmatrix} 0 \\ I \end{pmatrix}, \beta_3 = (I - \Sigma\Sigma^+) \begin{pmatrix} 0 \\ I \end{pmatrix}. \quad (32)$$

Remark: If matrices P, Q, R, S, H, N, J can be chosen according to (20), (25), (30), and (28), respectively, then, all conditions (8)-(12) are fulfilled.

III. UNIFIED \mathcal{H}_∞ OBSERVER DESIGN

As mentioned above, since the conditions (8)-(12) are satisfied, the system (7) is rewritten as follows:

$$\begin{cases} \dot{\zeta} &= \begin{pmatrix} N & M \\ P & G \end{pmatrix} \zeta - \begin{pmatrix} TB \\ 0 \end{pmatrix} \Delta\Phi \cdot u + \begin{pmatrix} JD_2 \\ QD_2 \end{pmatrix} \omega_n \\ e &= \begin{pmatrix} R & 0 \end{pmatrix} \zeta + SD_2\omega_n. \end{cases} \quad (33)$$

From the results of above parameterization, the matrices of system (33) can be rewritten as follows:

$$\mathbb{A}_1 = \begin{pmatrix} N & M \\ P & G \end{pmatrix} = A_{11} - ZA_{12} \quad (34)$$

$$\mathbb{B}_1 = \begin{pmatrix} JD_2 \\ QD_2 \end{pmatrix} = B_{11} - ZB_{12} \quad (35)$$

where $A_{11} = \begin{pmatrix} \alpha_3 & 0 \\ 0 & 0 \end{pmatrix}$, $Z = \begin{pmatrix} Y_{m3} & M \\ Y_{m1} & G \end{pmatrix}$, $A_{12} = \begin{pmatrix} \beta_1 & 0 \\ 0 & -I \end{pmatrix}$, $B_{11} = \begin{pmatrix} \Theta\Sigma^+ \begin{pmatrix} K \\ I_p \end{pmatrix} D_2 \\ 0 \end{pmatrix}$, $B_{12} = \begin{pmatrix} \beta_2 D_2 \\ 0 \end{pmatrix}$.

Note that estimation error e is independent of the matrix R . Since matrix Y_{m2} is fixed to $Y_{m2} = 0$, the following matrices are obtained

$$\mathbb{C}_1 = (R \ 0) = (\alpha_1 \ 0), \quad (36)$$

$$\mathbb{D}_1 = SD_2 = \alpha_2 D_2. \quad (37)$$

Besides, let denote

$$\mathbb{W}_1 = \begin{pmatrix} -TB \\ 0 \end{pmatrix}. \quad (38)$$

From these results (34)-(38), the estimation error dynamic system (33) becomes

$$\begin{cases} \dot{\zeta} &= \mathbb{A}_1\zeta + \mathbb{W}_1\Delta\Phi \cdot u + \mathbb{B}_1\omega_n \\ e &= \mathbb{C}_1\zeta + \mathbb{D}_1\omega_n. \end{cases} \quad (39)$$

Remark: All matrices A_{11} , A_{12} , B_{11} , B_{12} , \mathbb{W}_1 , \mathbb{C}_1 , \mathbb{D}_1 in the system (39) are known.

Assuming the Lipschitz condition (3) for $\Phi(x)$, the unified \mathcal{H}_∞ observer design problem is to determine the matrix Z such that:

- The system (39) is stable for $\omega_n(t) = 0$.
- $\|e(t)\|_{L_2} < \gamma \|\omega_n(t)\|_{L_2}$ for $\omega_n(t) \neq 0$.

The following theorem gives a sufficient condition to solve the above problem into an LMI framework

Theorem 1. Consider the system model (1) and the observer (4). Given positive scalars γ and ϵ_l . The above design problem is solved if there exist a symmetric positive definite matrix X and a matrix Y satisfying

$$\begin{bmatrix} \Omega_{11} & \Omega_{12} & \Omega_{13} \\ \Omega_{12}^T & -\epsilon_l I & 0 \\ \Omega_{13}^T & 0 & \epsilon_l U^T \mathbb{D}_1^T \Gamma^T \Gamma \mathbb{D}_1 U + \mathbb{D}_1^T \mathbb{D}_1 - \gamma^2 I \end{bmatrix} < 0 \quad (40)$$

where

$$\begin{aligned} \Omega_{11} &= A_{11}^T X - A_{12}^T Y^T + X A_{11} - Y A_{12} \\ &\quad + \epsilon_l U^T \mathbb{C}_1^T \Gamma^T \Gamma \mathbb{C}_1 U + \mathbb{C}_1^T \mathbb{C}_1, \end{aligned}$$

$$\Omega_{12} = X \mathbb{W}_1,$$

$$\Omega_{13} = X B_{11} - Y B_{12} + \epsilon_l U^T \mathbb{C}_1^T \Gamma^T \Gamma \mathbb{D}_1 U + \mathbb{C}_1^T \mathbb{D}_1,$$

the matrix Z will be then $Z = X^{-1}Y$.

Proof. Consider the following Lyapunov function candidate

$$V(t) = \zeta(t)^T X \zeta(t). \quad (41)$$

Differentiating $V(t)$ along the solution of (39) yields

$$\dot{V}(t) = \dot{\zeta}(t)^T X \zeta(t) + \zeta(t)^T X \dot{\zeta}(t). \quad (42)$$

For brevity, define $\eta = \begin{bmatrix} \zeta \\ \Delta\Phi \cdot u \\ \omega_n \end{bmatrix}$, then one obtains

$$\dot{V}(t) = \eta^T \mathbb{Q}_1 \eta \quad (43)$$

where $\mathbb{Q}_1 = \begin{bmatrix} \mathbb{A}_1^T X + X \mathbb{A}_1 & X \mathbb{W}_1 & X \mathbb{B}_1 \\ \mathbb{W}_1^T X & 0 & 0 \\ \mathbb{B}_1^T X & 0 & 0 \end{bmatrix}$.

From (3), the following condition is obtained

$$\Delta\Phi^T \Delta\Phi \leq e^T \Gamma^T \Gamma e. \quad (44)$$

From assumption A2, the inequality (44) implies

$$\begin{aligned} (\Delta\Phi u)^T \Delta\Phi u &\leq U^T (\mathbb{C}_1 \zeta + \mathbb{D}_1 \omega_n)^T \Gamma^T \Gamma (\mathbb{C}_1 \zeta + \mathbb{D}_1 \omega_n) U \\ &\Leftrightarrow \eta^T \mathbb{Q}_2 \eta \leq 0 \end{aligned} \quad (45)$$

where $\mathbb{Q}_2 = \begin{bmatrix} -U^T \mathbb{C}_1^T \Gamma^T \Gamma \mathbb{C}_1 U & 0 & -U^T \mathbb{C}_1^T \Gamma^T \Gamma \mathbb{D}_1 U \\ 0 & I & 0 \\ -U^T \mathbb{D}_1^T \Gamma^T \Gamma \mathbb{C}_1 U & 0 & -U^T \mathbb{D}_1^T \Gamma^T \Gamma \mathbb{D}_1 U \end{bmatrix}$.

In order to satisfy the objective design w.r.t. the \mathcal{L}_2 gain disturbance attenuation, the \mathcal{H}_∞ performance index is defined as:

$$\begin{aligned} J &= e^T e - \gamma^2 \omega_n^T \omega_n \\ &= \eta^T \mathbb{Q}_3 \eta \end{aligned} \quad (46)$$

where $\mathbb{Q}_3 = \begin{bmatrix} \mathbb{C}_1^T \mathbb{C}_1 & 0 & \mathbb{C}_1^T \mathbb{D}_1 \\ 0 & 0 & 0 \\ \mathbb{D}_1^T \mathbb{C}_1 & 0 & \mathbb{D}_1^T \mathbb{D}_1 - \gamma^2 I \end{bmatrix}$.

By applying the \mathcal{S} -procedure [18] to two constraints (44) and $J \geq 0$, $\dot{V}(t) < 0$ if there exist scalars $\epsilon_l > 0$, $\epsilon_n > 0$ such that

$$\begin{aligned} \dot{V}(t) - \epsilon_l (\eta^T \mathbb{Q}_2 \eta) + \epsilon_n J &< 0 \\ \Leftrightarrow \eta^T (\mathbb{Q}_1 - \epsilon_l \mathbb{Q}_2 + \epsilon_n \mathbb{Q}_3) \eta &< 0. \end{aligned} \quad (47)$$

The condition (47) is equivalent to

$$\mathbb{Q}_1 - \epsilon_l \mathbb{Q}_2 + \epsilon_n \mathbb{Q}_3 < 0. \quad (48)$$

In order to satisfy a sufficient condition to reject the measurement noise $\dot{V} + e^T e - \gamma^2 \omega_n^T \omega_n < 0$, ϵ_n is set to 1. The inequality (48) becomes:

$$\begin{aligned} &\mathbb{Q}_1 - \epsilon_l \mathbb{Q}_2 + \mathbb{Q}_3 < 0 \\ \Leftrightarrow &\begin{bmatrix} M_{11} & M_{12} & M_{13} \\ M_{12}^T & -\epsilon_l I & 0 \\ M_{13}^T & 0 & \epsilon_l U^T \mathbb{D}_1^T \Gamma^T \Gamma \mathbb{D}_1 U + \mathbb{D}_1^T \mathbb{D}_1 - \gamma^2 I \end{bmatrix} < 0 \end{aligned} \quad (49)$$

where $M_{11} = (\mathbb{A}_{11} - Z \mathbb{A}_{12})^T X + X (\mathbb{A}_{11} - Z \mathbb{A}_{12}) + \epsilon_l U^T \mathbb{C}_1^T \Gamma^T \Gamma \mathbb{C}_1 U + \mathbb{C}_1^T \mathbb{C}_1$,

$M_{12} = X \mathbb{W}_1$,

$M_{13} = X (\mathbb{B}_{11} - Z \mathbb{B}_{12}) + \epsilon_l U^T \mathbb{C}_1^T \Gamma^T \Gamma \mathbb{D}_1 U + \mathbb{C}_1^T \mathbb{D}_1$.

Let define $Y = XZ$ and substitute into (49), the LMI (40) is obtained.

If (40) is satisfied, (47) implies

$$\begin{aligned} \dot{V} + J < 0 &\Leftrightarrow \dot{V} < \gamma^2 \omega_n^T \omega_n - e^T e \\ &\Rightarrow \|e(t)\|_{\mathcal{L}_2}^2 < \gamma^2 \|\omega_n(t)\|_{\mathcal{L}_2}^2. \end{aligned} \quad (50)$$

The proof of Theorem 1 is completed. \square

Remark: If the observer matrices $M = 0$, $P = 0$, and $Q = 0$, the proposed observer become PI observer. In this case, Theorem 2.3.12 in [19] can be applied to find general solution of (40). The reader should refer [15] for more detailed.

IV. APPLICATION TO AUTOMOTIVE SUSPENSION

In this section, to assess the effectiveness of the proposed observer, it is applied to estimate the damper force in the automotive suspension system.

A. Semi-active suspension modeling

This section introduces the quarter-car model with the semi-active ER suspension system [1]. The well-known model consists of the sprung mass (m_s), the unsprung mass (m_{us}), the suspension components located between (m_s) and (m_{us}) and the tire which is modelled as a spring with stiffness k_t . From second law of Newton for motion, the system dynamics around the equilibrium are given as:

$$\begin{cases} m_s \ddot{z}_s &= -F_s - F_d \\ m_{us} \ddot{z}_{us} &= F_s + F_d - F_t \end{cases} \quad (51)$$

where $F_s = k_s(z_s - z_{us})$ is the spring force; $F_t = k_t(z_{us} - z_r)$ is the tire force; the damper force F_d is given as follows:

$$\begin{cases} F_d &= k_0(z_s - z_{us}) + c_0(\dot{z}_s - \dot{z}_{us}) + F_{er} \\ \dot{F}_{er} &= -\frac{1}{\tau} F_{er} + \frac{f_c}{\tau} \cdot u \cdot \tanh(k_1(z_s - z_{us})) \\ &+ c_1(\dot{z}_s - \dot{z}_{us}) \end{cases} \quad (52)$$

where, $c_0, c_1, k_0, k_1, f_c, \tau$ are constant parameters; z_s and z_{us} are the displacements of the sprung and unsprung masses, respectively. z_r is the road displacement input.

In the ER damper, control input u is the voltage input that provides the electrical field to control the ER damper. In practice, it is the duty cycle of the PWM signal that controls the application.

Moreover the measured outputs used in the observer real-time scheme are $y = [\ddot{z}_s, \ddot{z}_{us}]^T$, easily obtained from on board sensors (accelerometers).

By selecting the system states as $x = [x_1, x_2, x_3, x_4, x_5]^T = [z_s - z_{us}, \dot{z}_s, z_{us} - z_r, \dot{z}_{us}, F_{er}]^T \in \mathbb{R}^5$, and denoting $\omega_r = \dot{z}_r$ the road profile derivative and ω_n the sensor noises, the system dynamics in the state-space representation can be written as follows

$$\begin{cases} \dot{x} &= Ax + B\Phi(x)u + D_1\omega_r \\ y &= Cx + D_2\omega_n \end{cases} \quad (53)$$

where $\Phi(x) = \tanh(\Gamma x)$ with $\Gamma = [k_1 \quad c_1 \quad 0 \quad -c_1 \quad 0]$. Therefore, $\Phi(x)$ satisfies the Lipschitz condition (3).

The system matrices A, B, C, D_1, D_2 are known.

B. Synthesis results and frequency domain analysis

In the INOVE testbed available at GIPSA-lab, the control signal u (duty cycle of PWM signal) is limited in the range of $[0, 1]$. Therefore, applying Theorem 1, we obtain the \mathcal{L}_2 -induced gain $\gamma = 0.87$, $\epsilon_l = 50$, and the observer matrices N, J, H, M, P, Q, G, R and S .

The resulting attenuation of the sensor noises on the estimation error is shown in Figure 1. According to Figure 1, these results emphasize the effectiveness of the proposed observer in terms of noise rejection, since the upper bound on the singular values decreases rapidly in the region of high frequency noises.

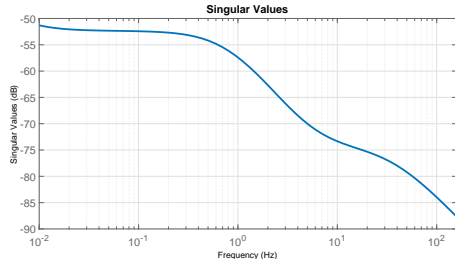


Fig. 1. Transfer $\|e/\omega_n\|$ - Upper bound on the singular value

C. Simulation

To emphasize the effectiveness of the proposed approach, simulations are done with the nonlinear quarter-car model (53). The initial conditions of the proposed design are as follows: $x_0 = [0, 0, 0, 0, 0, 0]^T$, $z_0 = [0.01, -0.4, 0.001, -0.15, 2]^T$, $v_0 = [0, 0, 0, 0, 0]^T$.

Three simulation scenarios are used to evaluate the performance of the observer as follows:

Scenario 1: It considers various road frequencies (from 0 Hz to 10 Hz)

- The road profile is a chirp signal
- The control input u is constant ($u = 0.35$)

Scenario 2: It considers a typical road profile

- An ISO 8608 road profile signal (Type C) is used.
- The control input u is constant ($u = 0.35$)

Scenario 3: It considers a closed-loop suspension control

- An ISO 8608 road profile signal (Type C) is used.

TABLE I

PARAMETER VALUES OF THE TESTBED MODEL

Parameter	Description	Value	Unit
m_s	Sprung mass	2.27	kg
m_{us}	unsprung mass	0.25	kg
k_s	Spring stiffness	1396	N/m
k_t	Tire stiffness	12270	N/m
k_0	Passive damper stiffness coefficient	170.4	N/m
c_0	Viscous damping coefficient	68.83	N.s/m
k_1	Hysteresis coefficient due to displacement	218.16	N.s/m
c_1	Hysteresis coefficient due to velocity	21	N.s/m
f_c	Dynamic yield force of ER fluid	28.07	N
τ	Time constant	43	ms

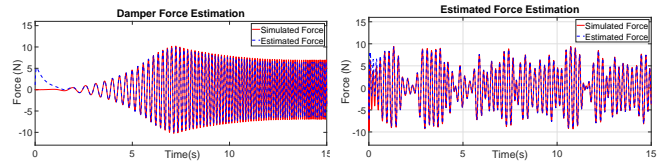


Fig. 2. (left) Simulation scenario 1, (right) Simulation scenario 2

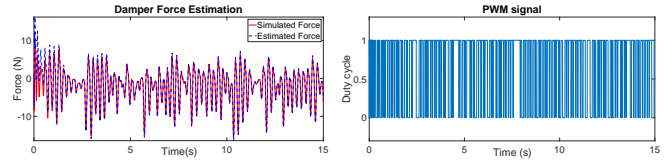


Fig. 3. Simulation scenario 3: (left) Damping force, (right) PWM signal

- Control input u is obtained from a Skyhook controller

The simulation results of three tests are shown in the Fig. 2 and Fig. 3. According to Fig. 2, the robustness of the unified observer to the frequency of road profile disturbance is guaranteed. It can be clearly observed that the damping force is estimated with a satisfactory accuracy at all frequencies of the road profile. In Fig. 3, the estimated result in a closed-loop control system test proves the efficiency in a realistic case.

D. Experimental validation

To validate the effectiveness of the proposed algorithm, real-time experiments have been performed on the 1/5 scaled car INOVE available at GIPSA-lab, shown in Fig. 4.

This test-bench which involves 4 semi-active ER suspensions is controlled in real-time using Matlab real-time workshop and a host computer. The target PC is connected to the host computer via Ethernet communication standard. The proposed observer system is implemented with the sampling period $T_s = 0.005s$. Note that the experimental platform is fully equipped with sensors to measure its vertical motion. At each corner of the system, a DC motor is used to generate the road profile.

The damping force estimation algorithm is applied for the rear-left corner using two sensors: the unsprung mass \ddot{z}_{us} and the sprung mass \ddot{z}_s accelerometers. For validation purpose only, the damper force sensor is used to compare the estimated force with the measured one.

Two experiment scenarios are used to validate the effectiveness of the proposed observer as follows:



Fig. 4. The experimental testbed INOVE at GIPSA-lab (see www.gipsa-lab.fr/projet/inove)

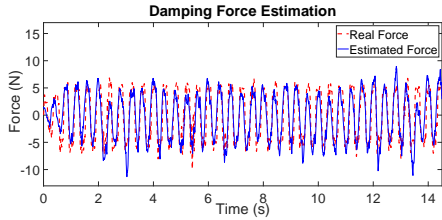


Fig. 5. Experiment 1: Damping force estimation

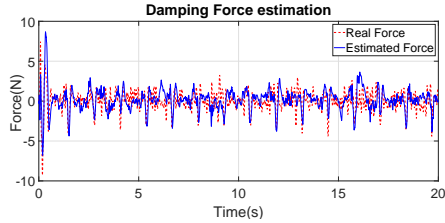


Fig. 6. Experiment 2: Damping force estimation

Experiment 1:

- The road profile is sequence of sinusoidal bumps
- The control input u is obtained from a Skyhook controller

Experiment 2:

- An ISO 8608 road profile signal (Type C) is used.
- The control input u is obtained from a Skyhook controller

The experiment results of the observer are presented in Fig. 5 and Fig. 6. The result illustrates the accuracy and efficiency of the proposed observer. To further describe this accuracy, Table II presents the normalized root-mean-square errors, considering the difference between the estimated and measured forces for experimental results presented in the Fig. 5 and Fig. 6.

V. CONCLUSION

This paper developed a unified \mathcal{H}_∞ observer to estimate the damper force, using a dynamic nonlinear model of the ER damper. For this purpose, the quarter-car system is represented in nonlinear Lipschitz form by considering a phenomenological damper model. Based on two accelerometers, the unified \mathcal{H}_∞ observer is designed, giving a good estimation result of the damping force. The estimation error is decoupled from the effect of unknown road profile and only minimized for the effect of measurement noises, while the nonlinearity term is bounded by a Lipschitz condition. Both simulation and experiment results assess the ability and the accuracy of the proposed model to estimate the damping force of the ER semi-active damper.

REFERENCES

[1] S. M. Savaresi, C. Poussot-Vassal, C. Spelta, O. Sename, and L. Dugard, *Semi-active suspension control design for vehicles*. Elsevier, 2010.

TABLE II
NORMALIZED ROOT-MEAN-SQUARE ERRORS (NRMSE)

Road Profile	NRMSE
Sinusoidal bumps	0.1108
ISO 8608 road	0.1392

[2] C. Poussot-Vassal, C. Spelta, O. Sename, S. M. Savaresi, and L. Dugard, "Survey and performance evaluation on some automotive semi-active methods: A comparative study on a single-corner model," *Annual Reviews in Control*, vol. 36, no. 1, pp. 148–160, 2012.

[3] C. Poussot-Vassal, O. Sename, L. Dugard, P. Gaspar, Z. Szabo, and J. Bokor, "A new semi-active suspension control strategy through LPV technique," *Control Engineering Practice*, vol. 16, no. 12, pp. 1519–1534, 2008.

[4] M.-Q. Nguyen, J. G. da Silva, O. Sename, and L. Dugard, "Semi-active suspension control problem: Some new results using an LPV/ H_∞ state feedback input constrained control," in *Decision and Control (CDC), 2015 IEEE 54th Annual Conference on*. IEEE, 2015, pp. 863–868.

[5] M. Fleps-Dezasse, F. Svaricek, and J. Brembeck, "Design and experimental assessment of an active fault-tolerant lpv vertical dynamics controller," *IEEE Transactions on Control Systems Technology*, 2018.

[6] G. Priyandoko, M. Mailah, and H. Jamaluddin, "Vehicle active suspension system using skyhook adaptive neuro active force control," *Mechanical systems and signal processing*, vol. 23, no. 3, pp. 855–868, 2009.

[7] G. Koch, T. Kloiber, and B. Lohmann, "Nonlinear and filter based estimation for vehicle suspension control," in *Decision and Control (CDC), 2010 49th IEEE Conference on*. IEEE, 2010, pp. 5592–5597.

[8] A. E. Vela, D. H. Alcántara, R. M. Menendez, O. Sename, and L. Dugard, " H_∞ observer for damper force in a semi-active suspension," *IFAC-PapersOnLine*, vol. 51, no. 11, pp. 764–769, 2018.

[9] J. C. Tudon-Martinez, D. Hernandez-Alcantara, O. Sename, R. Morales-Menendez, and J. d. J. Lozoya-Santos, "Parameter-dependent H_∞ filter for LPV semi-active suspension systems," *IFAC-PapersOnLine*, vol. 51, no. 26, pp. 19–24, 2018.

[10] R. Rajamani, "Observers for lipschitz nonlinear systems," *IEEE transactions on Automatic Control*, vol. 43, no. 3, pp. 397–401, 1998.

[11] A. Zemouche and M. Boutayeb, "On LMI conditions to design observers for lipschitz nonlinear systems," *Automatica*, vol. 49, no. 2, pp. 585–591, 2013.

[12] A. M. Pertew, H. J. Marquez, and Q. Zhao, " H_∞ observer design for Lipschitz nonlinear systems," *IEEE Transactions on Automatic Control*, vol. 51, no. 7, pp. 1211–1216, 2006.

[13] M. Darouach, L. Boutat-Baddas, and M. Zerrougui, " H_∞ observers design for a class of nonlinear singular systems," *Automatica*, vol. 47, no. 11, pp. 2517–2525, 2011.

[14] D. Koenig, "Observers design for unknown input nonlinear descriptor systems via convex optimization," *IEEE Transactions on Automatic control*, no. 06, pp. 1047–1052, 2006.

[15] N. Gao, M. Darouach, H. Voos, and M. Alma, "New unified H_∞ dynamic observer design for linear systems with unknown inputs," *Automatica*, vol. 65, pp. 43–52, 2016.

[16] N. Gao, M. Darouach, and M. Alma, "Dynamic observer design for a class of nonlinear systems," in *2018 IEEE 3rd Advanced Information Technology, Electronic and Automation Control Conference (IAEAC)*. IEEE, 2018, pp. 373–376.

[17] G. Phanomchoeng and R. Rajamani, "Observer design for Lipschitz nonlinear systems using riccati equations," in *American Control Conference (ACC), 2010*. IEEE, 2010, pp. 6060–6065.

[18] S. Boyd, L. El Ghaoui, E. Feron, and V. Balakrishnan, *Linear matrix inequalities in system and control theory*. Siam, 1994, vol. 15.

[19] R. E. Skelton, T. Iwasaki, and D. E. Grigoriadis, *A unified algebraic approach to control design*. CRC Press, 1997.